Chemical Engineering Journal 98 (2004) 199–211

Chemical Engineering Journal

www.elsevier.com/locate/cej

An integrated strategy for early detection of hazardous states in chemical reactors

Jyh-Shyong Chang*, Kui-Yi Chen

Department of Chemical Engineering, Tatung University, 40 Chungshan North Road, 3rd Sec., Taipei, Taiwan, ROC

Received 5 May 2003; accepted 31 July 2003

Abstract

To detect possible hazardous states occurring in a chemical reactor, the off-line parameter sensitivity analysis can be applied to ascertain whether the reactor system is operated in a parameter sensitive region. However, as the reactor is usually operated under closed-loop control in a real application, the off-line parameter sensitivity analysis was extended to the closed-loop operation of a batch reactor. It was found that if a closed-loop reactor system was operated in the parameter sensitive region, the maximal sensitivities of all state variables appeared at the same time. To avoid any possible measurement error of the initial concentration, a state observer was applied to provide correct states for the parameter sensitivity analysis under closed-loop operation. For the on-line detection of hazardous states, a neural network was built and applied to evaluate whether the operation conditions were located in the parameter sensitive region in the least computation time. Applicability of the developed integrated strategy for the early detection of hazardous states was demonstrated in batch reactors or continuously stirred tank reactors (CSTRs) using the acetic anhydride reaction catalyzed by sulfuric acid as the model reaction. Based on the prediction, in-time adjustments of operation conditions can be made to prevent any hazardous condition that might ensue in either a batch reactor or a continuously stirred tank reactor.

Keywords: Parameter sensitivity analysis; Hazardous states; Neural networks; State observer; Batch reactor; CSTR

1. Introduction

Batch reactors are one of the reactors that are extensively used in industry. Because of its flexibility and convenience in operation, batch reactors are always used in manufacturing products in small volume but of high added value. However, batch reactors are operated in a closed tank; improperly control may have other sub-reaction or cracking reaction not found in correct production. If out of control, reactors may reach high temperature and pressure beyond the endurance of the reactor, thus resulting in a runaway. Similar runaway phenomenon can be found in continuously stirred tank reactors (CSTRs). Therefore, problems concerning the design and operation of chemical reactors have been extensively discussed, resulting in numerous control and analysis methods. The technique of early detection of hazardous states in chemical reactors has been developed [1], like the On-Line Warning (OLIWA) system, which applies one-order and two-order differentiation of reaction temperature (dT/dt and d^2T/dt^2) to set up a safe operation detection system. Hugo et al. [2] concluded that as far as the safe operation problem in reaction is concerned, we do not want reactors to reach high temperature, which may end up with sub-reactions or cracking reactions and a possible runaway. Chemburkar et al. [3] proposed the generalized parametric sensitivity criterion to figure out a safe operation region for the steady state and multiple steady states in continuously stirred tank reactors. Morbidelli and Varma [4] applied the same method to find out the safe operation region for batch reactor operation. The generalized thermal parametric sensitivity criterion was applied to the thermal behavior of the esterification of 2-butanol with propionic anhydride in a batch reactor under isoperibolic conditions [5]. The last two works cited above studied this problem in an off-line way. Off-line parameter sensitivity analysis is inapplicable if the system parameters deviate from the assumed values; for example, the flow rate and inlet temperature of the cooling medium of the reactor system as well as the feed rate of the reactant are not kept at the desired values. As a reactor is usually operated under a temperature control loop, it is re-

Abbreviations: CSTR, continuously stirred tank reactor; PI, proportional-integral

* Corresponding author. Tel.: +886-2-5925252-3451; fax: +886-2-5861939.
E-mail address: jschang@ttu.edu.tw (J.-S. Chang).

1385-8947/$ – see front matter © 2003 Elsevier B.V. All rights reserved.
doi:10.1016/j.cej.2003.07.005

Nomenclature

A	heat transfer area (m^2)
$\boldsymbol{A}_r$	reduced order Jacobin matrix (Eq. (41))
B	heat of reaction dimensionless parameter (Eq. (30))
B^0	$B\varepsilon$ (Eq. (18))
B'	heat of reaction dimensionless parameter (Eq. (18))
$\boldsymbol{c}_r$	reduced order gradient vector (Eq. (41))
C	concentration of reactant ($kmol\,m^{-3}$)
C'	scaled concentration $(C - C_{min})/(C_{max} - C_{min})$
$\hat{C}$	estimated concentration of reactant ($kmol\,m^{-3}$)
C_p	mean specific heat ($kJ\,kg^{-1}\,K^{-1}$)
D_a	Damkohler number (Eq. (30))
e	estimation error
$\dot{\boldsymbol{e}}$	dynamic of estimation error
E	activation energy ($kJ\,kmol^{-1}\,K^{-1}$)
δf	modeling error
F	flow rate ($m^3\,s^{-1}$); federate (Eq. (1)); transformed function (Eq. (35))
$F_{i=1,2,3}$	function (Eqs. (19)–(21))
$F'_{i=1,2,3}$	function (Eqs. (26)–(28))
ΔH	heat of reaction ($kJ\,kmol^{-1}$)
$\boldsymbol{I}$	identity matrix
$\boldsymbol{J}$	Jacobian matrix of the system
k	reaction rate constant ($kmol\,m^{-3}\,s^{-1}$)
K_c	controller gain ($^\circ C^{-1}$)
L	observer gain
n	reaction order
P_3	dimensionless group (Eq. (30))
$P_{i=1,2}$	dimensionless groups (Eq. (18))
R	ideal gas constant ($kJ\,kmol^{-1}\,K^{-1}$); reaction rate
S_{t_b}	dimensionless heat transfer parameters (Eq. (30))
S_{t_c}	dimensionless heat transfer parameters (Eq. (30))
$\boldsymbol{s}_{\varphi_i}$	sensitivity matrix of states with respect to parameters
t	time (s)
t^*	time required for thermal runaway (s)
$\bar{t}$	dimensionless time (Eq. (18))
T	temperature ($^\circ C$ or K)
T'	scaled temperature $(T - T_{min})/(T_{max} - T_{min})$
$\bar{T}$	dimensionless temperature (Eq. (18))
u	controller output
U	overall heat transfer coefficient ($kJ\,K^{-1}\,s^{-1}$)
V	volume (m^3)
$\boldsymbol{x}$	vector of state variables
$\dot{\boldsymbol{x}}$	rate change of state vector
$\hat{\boldsymbol{x}}$	estimated vector of state variables
$\dot{y}$	rate change of measurement
z	dimensionless group (Eq. (18))

Greek letters

α_e	characteristic equation (Eq. (42))
γ	the inverse of dimensionless activation energy parameter (Eq. (30))
ε	dimensionless activation energy parameter (Eq. (18))
∇_{η_r}	gradient operator
$\boldsymbol{\eta}$	state vector to be estimated
$\dot{\boldsymbol{\eta}}$	rate change of state vector to be estimated
$\hat{\boldsymbol{\eta}}$	estimated state vector
$\dot{\hat{\boldsymbol{\eta}}}$	rate change of estimated state vector
λ	eigenvalue of characteristic equation
ρ	density ($kg\,m^{-3}$)
τ	dimensionless heat transfer parameter (Eq. (18))
τ'	dimensionless space time (Eq. (30))
τ_I	intergral time of the PI controller (s)
ϕ	vector of parameters
ψ	Semenov number (Eq. (18))
ψ^0	dimensionless parameter (Eq. (18))

Subscripts

A	component A
b	batch side
c	cooling water
i	individual
in	inlet
max	maximal
min	minimal
r	reduced order
ref	reference
S	sulfuric acid as catalyst
0	initial; inlet

Superscript

$*$	desired; time required for thermal runaway

warding to develop an on-line parameter sensitivity analysis for an early detection of hazardous states of the reacting medium under closed-loop operation. In order to provide the parameter sensitivity analysis with correct states, Alós et al. [6] discussed the application of a model-based estimation technique, namely a Kalman filter, to the on-line detection of hazardous states in the transients of a continuous process. The detection system developed by Alós et al. [6] can identify the hazardous start-up 9 min before the excursion takes place in case of an initial mischarge of the catalyst. However, the reactor system studied by Alós et al. [6] seemed to be an open-loop one, unable to reflect the real world situation properly.

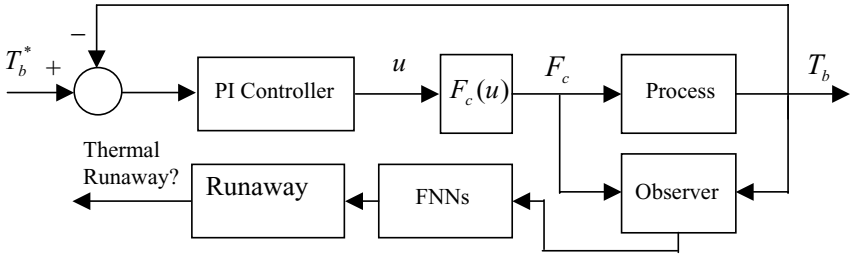

Fig. 1. Structure of an observer/FNNs based early detection system.

In this work, both the kinetic data and the related system parameters were assumed properly available. Based on the available process model and parameters, we built a database which was composed of the inputs, the loading of the reactants, and the initial temperature of reaction, as well as the outputs, the thermal runaway index, and the time for thermal runaway, by the off-line parameter sensitivity analysis. For on-line application, interpolation of the built database was required to save the on-line computation time for the integration of dynamic equations governing the parameter sensitivity analysis. Therefore, a feed-forward neural network (FNN) was built to give the mapping between the inputs and outputs of the database. To obtain a correct result from the parameter sensitivity analysis, an effective observer was developed to provide the parameter sensitivity analysis with the correct states. Thus, the correct thermal runaway index and the time for thermal runaway could be calculated form the built FNN, the reactor could be predicted whether it was in the parametric sensitive space, and suitable adjustment of the operation conditions could be proposed to avoid any possible dangerous accident in due time. The integrated scheme proposed is depicted in Fig. 1.

2. The process

In this work, the sulfuric acid-catalyzed hydrolysis of acetic anhydride reaction was adopted as the model reaction.

$$(CH_3CO)_2O + H_2O \xrightarrow{H_2SO_4} 2CH_3COOH$$

The reaction was carried out either in a jacketed batch reactor or in a jacketed CSTR. The conventional proportional-integral (PI) controller adjusted the flow rate of the coolant through the jacket side. The mass and energy balance equations are

$$\frac{dC_A}{dt} = \frac{F}{V_b}(C_{Af} - C_A) - R_A \quad (1)$$

$$\frac{dT_b}{dt} = \frac{F}{V_b}(T_f - T_b) + \frac{-\Delta H}{C_{pb}\rho_b}R_A + \frac{UA}{V_b C_{pb}\rho_b}(T_c - T_b) \quad (2)$$

$$\frac{dT_c}{dt} = \frac{UA}{V_c\rho_c C_{pc}}(T_b - T_c) + \frac{F_c}{V_c}(T_{cin} - T_c) \quad (3)$$

$$R_A = k_0\, e^{-E/R(T_b+273.15)} C_A C_s \quad (4)$$

with initial conditions

$$C_A = C_{A_0}, \qquad T_b = T_{b_0}, \qquad T_c = T_{c_0} \quad (5)$$

The PI controller adjusts the flow rate of the coolant by

$$F_c = (F_{c_{min}} - F_{c_{max}})u + F_{c_{max}} \quad (6)$$

$$u(t) = K_c e(t) + \frac{K_c}{\tau_1}\int_0^t e(\tau)\,d\tau + \text{bias} \quad (7)$$

$$e(t) = T_b^*(t) - T_b(t) \quad (8)$$

The controller output is constrained

$$u_{min} \le u(t) \le u_{max}$$

$$u_{min} = 0, \qquad u_{max} = 1$$

$$F_{c_{min}} = 0, \qquad F_{c_{max}} = 2.5 \times 10^{-4}\,m^3\,s^{-1} \quad (9)$$

The relation of U and F_c is

$$U = a_0 + a_1 F_c \quad (10)$$

where $a_0 = 0.12$; $a_1 = 1.14 \times 10^3$.

If the external feed rate $F = 0$, the reactor is operated in a batch mode; otherwise, the reactor is operated in a CSTR mode.

3. Parametric sensitivity analysis

To remove the drawback of the criterion [7] specific to the process studied, Morbidelli and Varma [4] presented an intrinsic criterion based on a generalized behavior of the sensitivities of the states with respect to the operating conditions. It is expected to recognize if a process is becoming dangerous.

A differential equation of describing the dynamic behavior in a chemical reactor

$$\frac{d\boldsymbol{y}}{dx} = \boldsymbol{F}(x, \boldsymbol{y}, \boldsymbol{\phi}) \quad (11)$$

$\boldsymbol{y}$ is the vector of a dependent variable (temperature or concentration), x is an independent variable (time), $\boldsymbol{\phi}$ represents the input parameters of the system. The elements of the first-order sensitivity coefficient matrix are defined as:

$$s_{j,\phi_i} = \frac{dy_j}{d\phi_i} \quad (12)$$

By directly differentiating Eq. (11), one can obtain the following:

$$\frac{\mathrm{d}\boldsymbol{s}_{\phi_i}}{\mathrm{d}x} = J s_{\phi_i} + \frac{\partial \boldsymbol{F}(x, y, \boldsymbol{\phi})}{\partial \phi_i} \tag{13}$$

where $\boldsymbol{J}$ is the Jcobian matrix of the system. The initial conditions for Eq. (13) are

$$s_{\phi_i} = 0 \text{ at } x = 0$$

3.1. Parametric sensitivity analysis for the open-loop batch reactor system

By transforming the governing equations of the batch reactor system into the dimensionless design equations for the process considered, one can obtain:

$$\frac{\mathrm{d}\bar{T}_b}{\mathrm{d}\bar{t}} = \varepsilon(1-z)^n f(\bar{T}_b) + \frac{\varepsilon}{\psi^0}(\bar{T}_c - \bar{T}_b) \tag{14}$$

$$\frac{\mathrm{d}\bar{T}_c}{\mathrm{d}\bar{t}} = \frac{\varepsilon P_1}{\psi^0}(\bar{T}_b - \bar{T}_c) + 2P_2(\bar{T}_{cin} - \bar{T}_c) \tag{15}$$

$$\frac{\mathrm{d}z}{\mathrm{d}\bar{t}} = \frac{\varepsilon}{B^0}(1-z)^n f(\bar{T}_b) \tag{16}$$

The initial condition is

$$z = 0, \qquad \bar{T}_b = \bar{T}_{b_0}, \qquad \bar{T}_c = \bar{T}_{c_0} \quad \text{at } \bar{t} = 0 \tag{17}$$

where

$$f(\bar{T}_b) = \mathrm{e}^{\varepsilon(1-(1/\bar{T}_b + (273.15/T_{ref})))};$$

$$\psi = \frac{(-\Delta H)k(T_{ref}){C_{A_0}}^n C_s V_b}{T_{ref}\varepsilon UA};$$

$$k(T_{ref}) = k_0\,\mathrm{e}^{-(E/RT_{ref})}; \qquad B = \frac{(-\Delta H)C_{A_0}C_s}{C_{pb}\rho_b T_{ref}\varepsilon}$$

$$\varepsilon = \frac{E}{RT_{ref}}; \qquad P_1 = \frac{V_b\rho_b C_{pb}}{V_c\rho_c C_{pc}};$$

$$P_2 = \frac{T_{ref}\varepsilon\rho_b C_{pb}F_c}{(-\Delta H)k(T_{ref}){C_{A_0}}^n C_s V_c} \tag{18}$$

$$B^0 = B\varepsilon; \qquad \psi^0 = \psi\varepsilon; \qquad \bar{T}_b = \frac{T_b}{T_{ref}};$$

$$\bar{T}_c = \frac{T_c}{T_{ref}}; \qquad z = \frac{C_{A_0} - C_A}{C_{A_0}}; \qquad \bar{t} = \psi\tau;$$

$$\tau = \frac{UA}{C_{pb}\rho_b V_b}t$$

In order to observe the real states, the following equations can be derived from Eqs. (14)–(16).

$$\frac{\mathrm{d}T_b}{\mathrm{d}t} = AT_{ref}\left[\varepsilon(1-z)^n f\left(\frac{T_b}{T_{ref}}\right) + \frac{\varepsilon}{\psi^0}\left(\frac{T_c}{T_{ref}} - \frac{T_b}{T_{ref}}\right)\right] = F_1 \tag{19}$$

$$\frac{\mathrm{d}T_c}{\mathrm{d}t} = AT_{ref}\left[\frac{\varepsilon P_1}{\psi^0}\left(\frac{T_b}{T_{ref}} - \frac{T_c}{T_{ref}}\right) + 2P_2\left(\frac{T_{cin}}{T_{ref}} - \frac{T_c}{T_{ref}}\right)\right] = F_2 \tag{20}$$

$$\frac{\mathrm{d}z}{\mathrm{d}t} = A\left[\frac{\varepsilon}{\beta^0}(1-z)^n f\left(\frac{T_b}{T_{ref}}\right)\right] = F_3 \tag{21}$$

where

$$f\left(\frac{T_b}{T_{ref}}\right) = \mathrm{e}^{\varepsilon(1/(T_b/T_{ref}) + (273.15/T_{ref}))} \tag{22}$$

$$A = \frac{(-\Delta H)k_0\,\mathrm{e}^{-\varepsilon}{C_{A_0}}^n C_s}{T_{ref}\varepsilon\rho_b C_{pc}} \tag{23}$$

The dynamic equation for parameter sensitivity is

$$\frac{\mathrm{d}\boldsymbol{s}_{y\phi_i}}{\mathrm{d}t} = \frac{\mathrm{d}\begin{bmatrix} \frac{\mathrm{d}T_b}{\mathrm{d}\phi_i} \\ \frac{\mathrm{d}T_c}{\mathrm{d}\phi_i} \\ \frac{\mathrm{d}z}{\mathrm{d}\phi_i} \end{bmatrix}}{\mathrm{d}t} = \begin{bmatrix} \frac{\partial F_1}{\partial T_b} & \frac{\partial F_1}{\partial T_c} & \frac{\partial F_1}{\partial z} \\ \frac{\partial F_2}{\partial T_b} & \frac{\partial F_2}{\partial T_c} & \frac{\partial F_2}{\partial z} \\ \frac{\partial F_3}{\partial T_b} & \frac{\partial F_3}{\partial T_c} & \frac{\partial F_3}{\partial z} \end{bmatrix} \begin{bmatrix} \frac{\mathrm{d}T_b}{\mathrm{d}\phi_i} \\ \frac{\mathrm{d}T_c}{\mathrm{d}\phi_i} \\ \frac{\mathrm{d}z}{\mathrm{d}\phi_i} \end{bmatrix} + \begin{bmatrix} \frac{\partial F_1}{\partial \phi_i} \\ \frac{\partial F_2}{\partial \phi_i} \\ \frac{\partial F_3}{\partial \phi_i} \end{bmatrix} \tag{24}$$

where $\phi_i = \{\psi^0,\ B^0,\ n,\ \varepsilon,\ P_1,\ P_2\}$.

The initial condition

$$s_{y\phi_i} = 0 \quad \text{at } t = 0 \tag{25}$$

Given the system parameters shown in Table 1 and the initial conditions shown in Table 2, the behavior of the parameter sensitivities $s_{y\phi_i}$, for each of the six independent parameters of the model, is shown in Figs. 2 and 3. In these two figures,

Table 1
System parameters of sulfuric acid-catalyzed hydrolysis of acetic anhydride reaction in the batch reactor and CSTR

V_b (m^3)	0.0082
ρ_b ($kg\,m^{-3}$)	1000
C_{pb} ($kJ\,kg^{-1}\,K^{-1}$)	3.862
V_c (m^3)	0.0011
ρ_c ($kg\,m^{-3}$)	1000
C_{pc} ($kJ\,kg^{-1}\,K^{-1}$)	4.184
C_s ($kmol\,m^{-3}$)	0.225
F ($m^3\,s^{-1}$)[a]	5×10^{-4}
T_{cin} (°C)	20
k_0 ($m^3\,kmol^{-1}\,s^{-1}$)	1.85×10^{14}
E/R (K)	11244
ΔH ($kJ\,kmol^{-1}$)	-1.741×10^5
T_{ref} (K)	298
F_c ($m^3\,s^{-1}$)	1.25×10^{-4}
T_{c_0} (°C)	20

[a] For CSTR operation (the other parameters are used for both batch reactor and CSTR operation).

Table 2
The operating conditions of the reactor systems

T_{b_0} (°C)	C_{A_0} (kmol m^{-3})	Figure
50	1	Fig. 2
50	3	Fig. 3
20	3	Figs. 10 and 11

the peaks of $s_{T_c\phi_i}$ are not significant compared with those of $s_{T_b\phi_i}$ and $s_{z_{\phi_i}}$; therefore, there are not depicted in the figures. Similar results to those available from the work of Morbidelli and Varma [4] were obtained. Note that for the safe condition ($C_{A_0} = 1\,\text{kmol m}^{-3}$) the sensitivities present the peak at different times, whereas in runaway conditions (higher dosing of acetic anhydride, $C_{A_0} = 3\,\text{kmol m}^{-3}$) the maxima appear distinctly at the same time, regardless of the particular state variable or the particular parameter chosen for the definition of the sensitivity. An interval of 0.1 s is chosen to measure the closeness of the peaks in time, clearly indicating the intrinsic nature of the sensitivity criterion proposed by Morbidelli and Varma [4] and allows one to define a unique region of the parameter space where the model becomes sensitive to small variations of any of its independent input parameters.

3.2. Parametric sensitivity analysis for the open-loop CSTR system

For the CSTR system, the following equations similar to those of Eqs. (19)–(21) can be derived:

$$\frac{dT_b}{dt} = \frac{T_{ref}}{\tau'}\left[\left(\frac{T_f}{T_{ref}} - \frac{T_b}{T_{ref}}\right) + S_{t_b}\left(\frac{T_c}{T_{ref}} - \frac{T_b}{T_{ref}}\right) + B'\gamma D_a\, e^{1/\gamma(1-(T_{ref}/T))}(1-z)\right] = F_1' \quad (26)$$

$$\frac{dT_c}{dt} = \frac{T_{ref}}{\tau'}\left[S_{t_c}\left(\frac{T_b}{T_{ref}} - \frac{T_c}{T_{ref}}\right) + P_3\left(\frac{T_{cin}}{T_{ref}} - \frac{T_c}{T_{ref}}\right)\right] = F_2' \quad (27)$$

$$\frac{dz}{dt} = \frac{1}{\tau'}\left[-z + D_a\, e^{1/\gamma(1-(1/T_b/T_{ref}))}(1-z)\right] = F_3' \quad (28)$$

The initial condition is

$$z = 0, \qquad T_b = T_{b_0}, \qquad T_c = T_{c_0} \quad \text{at } t = 0, \quad (29)$$

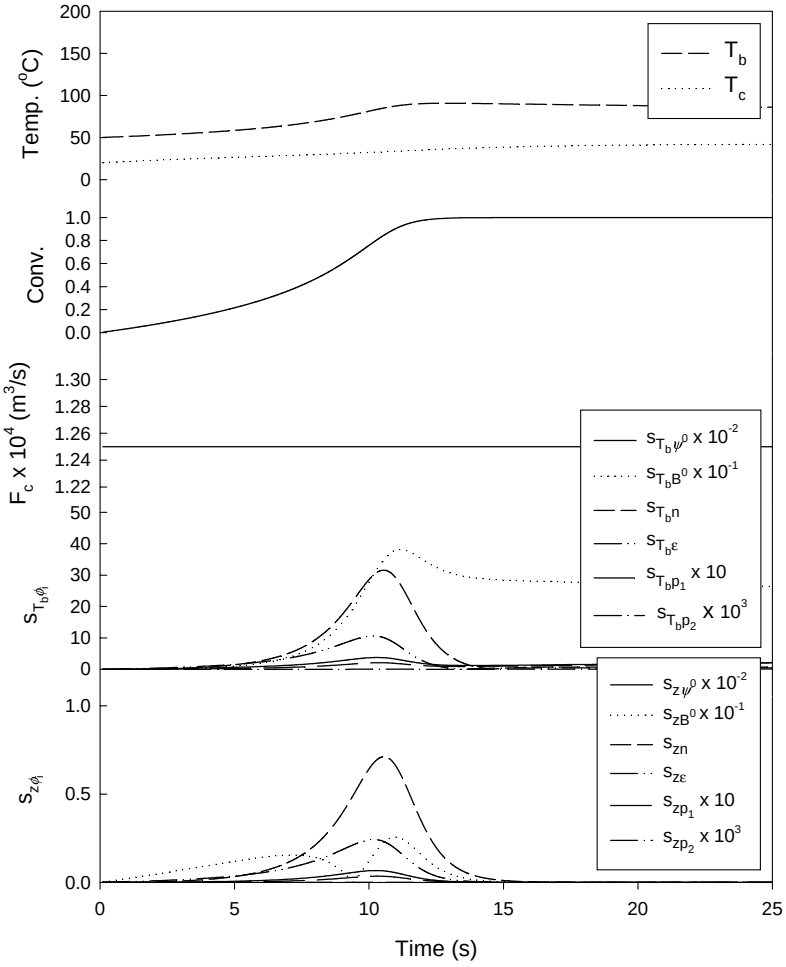

Fig. 2. Time profiles of T_b, T_c, z, $s_{T_b\varphi_i}$, $s_{z\varphi_i}$ ($T_{b_0} = 50\,°\text{C}$, $C_{A_0} = 1\,\text{kg m}^{-3}$) developing in the batch reactor.

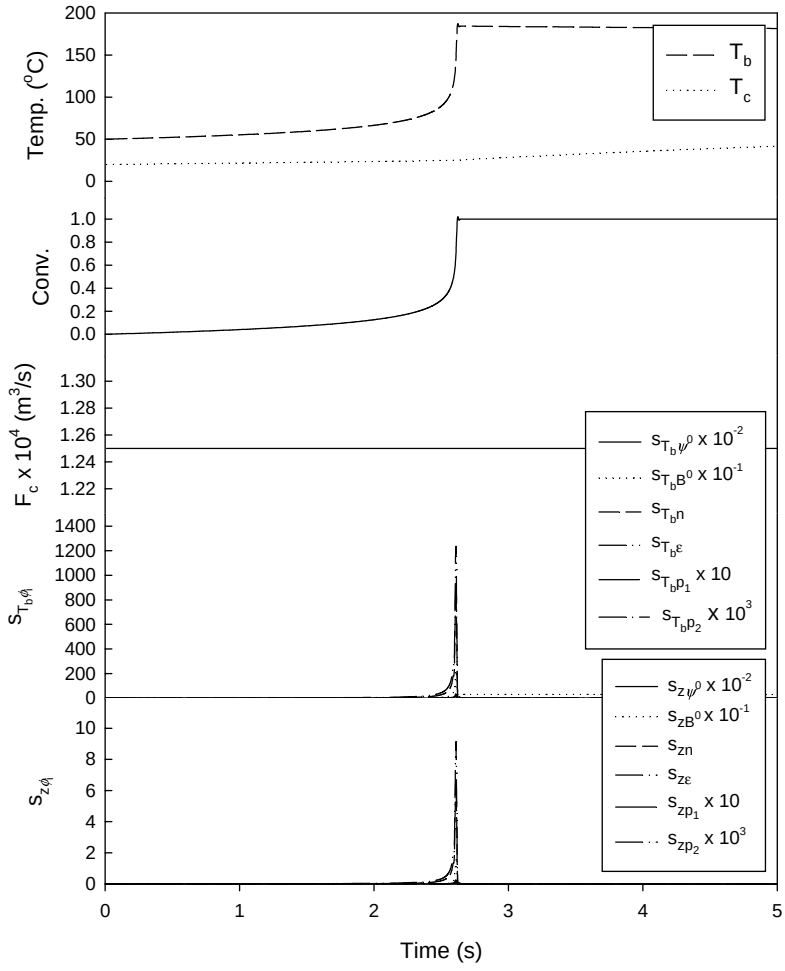

Fig. 3. Time profiles of T_b, T_c, z, $s_{T_b\varphi_i}$, $s_{z_{\varphi_i}}$ ($T_{b_0} = 50\,^\circ\mathrm{C}$, $C_{A_0} = 3\ \mathrm{kg\,m^{-3}}$) developing in the batch reactor.

where

$$\gamma = \frac{RT_{\mathrm{ref}}}{E}; \qquad \tau' = \frac{V_b}{F}; \qquad D_a = k_0\,\mathrm{e}^{-(1/\gamma)}\tau'$$

$$S_{t_b} = \frac{UA\tau'}{\rho_b C_{pb} V_b}; \qquad S_{t_c} = \frac{UA\tau'}{\rho_c C_{pc} V_c};$$

$$B' = \frac{(-\Delta H)C_{Af}}{\rho_b C_{pb} T_{\mathrm{ref}}\gamma}; \qquad P_3 = \frac{F_c\tau'}{V_c} \tag{30}$$

The dynamic equation for parameter sensitivity is

$$\frac{\mathrm{d}\boldsymbol{s}_{y\varphi_i}}{\mathrm{d}t} = \frac{\mathrm{d}\begin{bmatrix} \frac{\mathrm{d}T_b}{\mathrm{d}\phi_i} \\ \frac{\mathrm{d}T_c}{\mathrm{d}\phi_i} \\ \frac{\mathrm{d}z}{\mathrm{d}\phi_i} \end{bmatrix}}{\mathrm{d}t} = \begin{bmatrix} \frac{\partial F_1'}{\partial T_b} & \frac{\partial F_1'}{\partial T_c} & \frac{\partial F_1'}{\partial z} \\ \frac{\partial F_2'}{\partial T_b} & \frac{\partial F_2'}{\partial T_c} & \frac{\partial F_2'}{\partial z} \\ \frac{\partial F_3'}{\partial T_b} & \frac{\partial F_3'}{\partial T_c} & \frac{\partial F_3'}{\partial z} \end{bmatrix} \begin{bmatrix} \frac{\mathrm{d}T_b}{\mathrm{d}\phi_i} \\ \frac{\mathrm{d}T_c}{\mathrm{d}\phi_i} \\ \frac{\mathrm{d}z}{\mathrm{d}\phi_i} \end{bmatrix} + \begin{bmatrix} \frac{\partial F_1'}{\partial \phi_i} \\ \frac{\partial F_2'}{\partial \phi_i} \\ \frac{\partial F_3'}{\partial \phi_i} \end{bmatrix} \tag{31}$$

where $\phi_i = \{D_a,\ S_{t_b}, B',\ \gamma,\ S_{t_c},\ P_3\}$.The initial condition

$$s_{y\phi_i} = 0 \qquad \text{at } t = 0 \tag{32}$$

Given the system parameters and the initial conditions of the CSTR as shown in Tables 1 and 2, the behavior of the parameter sensitivities $s_{y\phi_i}$ for each of the six independent parameters of the model similar to those indicated in Figs. 2 and 3 is not provided here for brevity.

3.3. Parametric sensitivity analysis for the closed-loop reaction systems

Extension of the parametric sensitivity analysis from the open-loop reaction system to the closed-loop reaction system using a PI controller is straightforward. It is proper to assume that the process is operated in a thermal safe condition if the manipulated variable (the adjusting coolant) is not stuck at the lower or upper bound ($F_{c_{min}}$ or $F_{c_{max}}$). Therefore, if the reactor is operated in the thermal safe condition, each of the first-order sensitivity coefficients is set to be zero while integrating the sensitivity analysis equations. If $F_c = F_{c_{min}}$ or $F_c = F_{c_{max}}$, then the analysis is the same as that done in the open-loop operation.

4. Determination of sensitivity parameter space via FNNs

If the batch reactor is operated at $F_c = F_{c_{min}}$ or $F_c = F_{c_{max}}$, the required dimensionless parameters shown in Eq. (18) for the parametric sensitivity analysis will be only a function of T_{b_0} and C_{A_0}. Therefore, the possible operating region of the process T_{b_0} (°C) ∈ [50 85], C_{A_0} (kmol m^{-3}) ∈ [0.5 5.], and $\Delta T_{b_0} = 2.5\,^{\circ}$C; $\Delta C_{A_0} = 0.5$ kmol m^{-3}, a set of 300 different combinations of initial conditions were designed to do the parametric sensitivity analysis. The collected data T_{b_0} and C_{A_0} were adopted as the inputs of the networks while the thermal runaway index ($a = 0$ for thermal safe operation; $a = 1$ for thermal runaway) and the time for thermal runaway t^* were adopted as the outputs of the networks. These two FNNs as shown in Fig. 4 were chosen to represent the mapping between the inputs and the outputs. The recall data for the trained FNNs are shown in Figs. 5 and 6. In Figs. 4–6, T'_{b_0} and C'_{A_0} are scaled values of T_{b_0} and C_{A_0}, respectively. These two FNNs were well trained; interpolations of these two FNNs were also satisfied but not included in the content. Based on these two FNNs, one can determine whether and when the reacting medium is going to be a thermal runaway given the initial operating conditions. Another set of FNNs for the CSTR was also built for application.

5. Nonlinear state observer with variable gain

In order to control the decay speed of the estimation error, the nonlinear observer with constant observer gain developed by Soroush [8] was extended to a design with variable gain. Consider the following multi-input/single-output (MISO) nonlinear system below:

$$\begin{aligned} \dot{\boldsymbol{x}} &= \boldsymbol{f}(\boldsymbol{x}, \boldsymbol{u}) \\ y &= x_n \end{aligned} \tag{33}$$

where $\boldsymbol{x} = [x_1, x_2, \ldots, x_n]^{\mathrm{T}}$ is a state vector and $\boldsymbol{u}$ is the external inputs. The function Eq. (26) is subject to a norm-bounded modeling error δf_i. Eq. (33) can be written in the form of Eq. (34) as:

$$\begin{aligned} \dot{\boldsymbol{\eta}} &= \boldsymbol{F}_{\boldsymbol{\eta}}(\boldsymbol{\eta}, y, \boldsymbol{u}) \\ \dot{y} &= F_y(\boldsymbol{\eta}, y, \boldsymbol{u}) \end{aligned} \tag{34}$$

where

$$\begin{aligned} F_{\eta_i}(\boldsymbol{\eta}, y, \boldsymbol{u}) &= f_i(\boldsymbol{x}, \boldsymbol{u}) \quad i = 1\text{–}n-1 \\ F_y(\boldsymbol{\eta}, y, \boldsymbol{u}) &= f_n(\boldsymbol{x}, \boldsymbol{u}) \end{aligned} \tag{35}$$

The closed-loop, reduced-order observer becomes

$$\begin{aligned} \dot{\hat{\boldsymbol{\eta}}} &= \boldsymbol{F}_{\boldsymbol{\eta}}(\hat{\boldsymbol{\eta}}, \boldsymbol{y}, \boldsymbol{u}) + \boldsymbol{L}[\dot{y} - F_y(\hat{\boldsymbol{\eta}}, y, \boldsymbol{u})] \\ \hat{x} &= \hat{\boldsymbol{\eta}} \end{aligned} \tag{36}$$

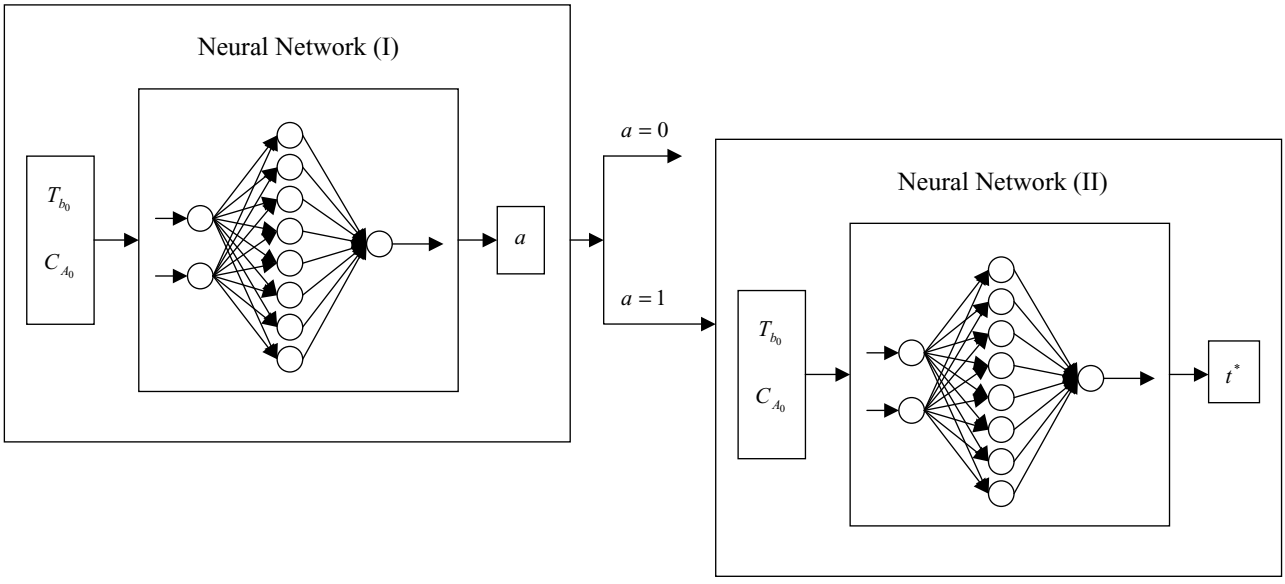

Fig. 4. The neural network structure for mapping the inputs and outputs of the parametric sensitivity analysis for the batch reactor system.

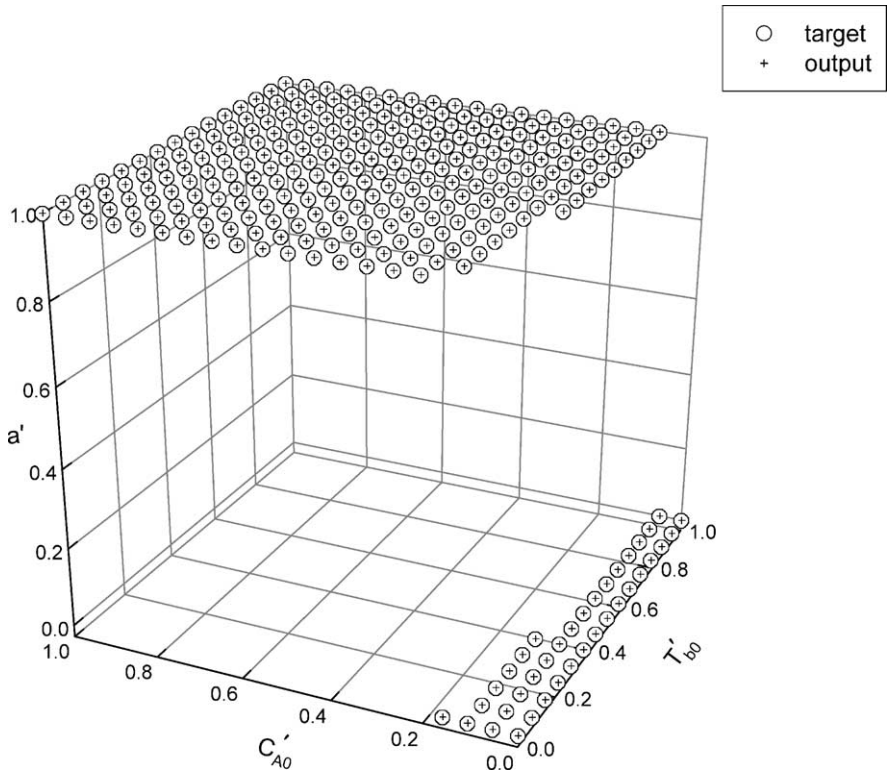

Fig. 5. Performance of the recall of the built FNN for *a* for the batch reactor system.

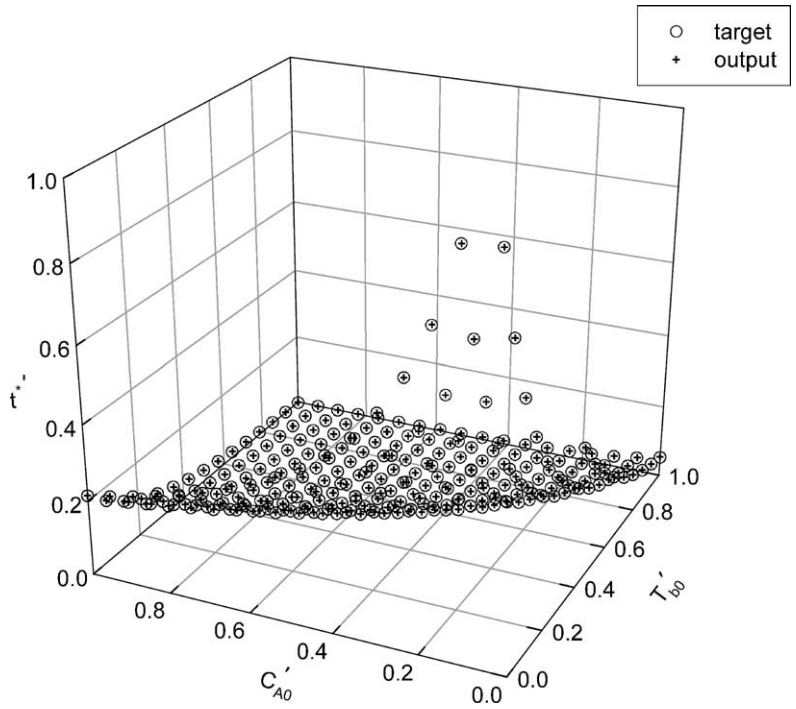

Fig. 6. Performance of the recall of the built FNN for t^* for the batch reactor system.

The corresponding observer error dynamics are governed by

$$\dot{e} = \boldsymbol{F}_{\boldsymbol{\eta}}(\mathrm{e}+\eta, y, \boldsymbol{u}) - \boldsymbol{F}_{\boldsymbol{\eta}}(\boldsymbol{\eta}, y, \boldsymbol{u}) - \boldsymbol{L}\{F_y(e+\boldsymbol{\eta}, y, \boldsymbol{u}) - F_y(\boldsymbol{\eta}, \mathrm{y}, \boldsymbol{u})\} \quad (37)$$

The above equation is composed of the following equations

$$\begin{aligned}
\dot{e}_1 &= \Delta f_1 + \delta f_1 - L_1(\Delta f_n + \delta f_n)\\
\dot{e}_2 &= \Delta f_2 + \delta f_2 - L_2(\Delta f_n + \delta f_n)\\
&\vdots\\
\dot{e}_{n-1} &= \Delta f_{n-1} + \delta f_{n-1} - L_{n-1}(\Delta f_n + \delta f_n)
\end{aligned} \quad (38)$$

By linearizing locally with respect to the estimated states $\hat{\boldsymbol{\eta}}$, Eq. (13) can be treated as a state observer with the following form:

$$\begin{aligned}
\dot{e}_1 &= \left\{\frac{\partial f_1}{\partial \eta_1} - L_1\frac{\partial f_n}{\partial \eta_1}\right\} e_1 + \cdots + \left\{\frac{\partial f_1}{\partial \eta_{n-1}} - L_1\frac{\partial f_n}{\partial \eta_{n-1}}\right\} e_{n-1} + (\delta f_1 - L_1\delta f_n)\\
\dot{e}_2 &= \left\{\frac{\partial f_2}{\partial \eta_1} - L_2\frac{\partial f_n}{\partial \eta_1}\right\} e_1 + \cdots + \left\{\frac{\partial f_2}{\partial \eta_{n-1}} - L_2\frac{\partial f_n}{\partial \eta_{n-1}}\right\} e_{n-1} + (\delta f_2 - L_2\delta f_n)\\
&\vdots\\
\dot{e}_{n-1} &= \left\{\frac{\partial f_{n-1}}{\partial \eta_1} - L_{n-1}\frac{\partial f_n}{\partial \eta_1}\right\} e_1 + \cdots + \left\{\frac{\partial f_{n-1}}{\partial \eta_{n-1}} - L_{n-1}\frac{\partial f_n}{\partial \eta_{n-1}}\right\} e_{n-1} + (\delta f_{n-1} - L_{n-1}\delta f_n)
\end{aligned} \quad (39)$$

We ignore the structural modeling error terms and let

$$\dot{e}_{\mathrm{r}} = \begin{bmatrix} \dot{e}_1 \\ \dot{e}_2 \\ \vdots \\ \dot{e}_{n-1} \end{bmatrix} = \boldsymbol{H}(\hat{\eta}) \begin{bmatrix} e_1 \\ e_2 \\ \vdots \\ e_{n-1} \end{bmatrix} \quad (40)$$

where $\boldsymbol{e}_{\mathrm{r}} \in \boldsymbol{R}^{n-1}$ and

$$\begin{aligned}
\boldsymbol{H}(\hat{\boldsymbol{\eta}}) &= \begin{bmatrix} \frac{\partial f_1}{\partial \eta_1} - L_1\frac{\partial f_n}{\partial \eta_1} & \cdots & \frac{\partial f_1}{\partial \eta_{n-1}} - L_1\frac{\partial f_n}{\partial \eta_{n-1}} \\ \frac{\partial f_2}{\partial \eta_1} - L_2\frac{\partial f_n}{\partial \eta_1} & \cdots & \frac{\partial f_2}{\partial \eta_{n-1}} - L_2\frac{\partial f_n}{\partial \eta_{n-1}} \\ \vdots & \ddots & \vdots \\ \frac{\partial f_{n-1}}{\partial \eta_1} - L_{n-1}\frac{\partial f_n}{\partial \eta_1} & \cdots & \frac{\partial f_{n-1}}{\partial \eta_{n-1}} - L_{n-1}\frac{\partial f_n}{\partial \eta_{n-1}} \end{bmatrix}\\
&= \begin{bmatrix} \frac{\partial f_1}{\partial \eta_1} & \cdots & \frac{\partial f_1}{\partial \eta_{n-1}} \\ \vdots & \ddots & \vdots \\ \frac{\partial f_{n-1}}{\partial \eta_1} & \cdots & \frac{\partial f_{n-1}}{\partial \eta_{n-1}} \end{bmatrix} - \begin{bmatrix} L_1 \\ \vdots \\ L_{n-1} \end{bmatrix} \times \begin{bmatrix} \frac{\partial f_n}{\partial \eta_1} \cdots \frac{\partial f_n}{\partial \eta_{n-1}} \end{bmatrix}\\
&\triangleq \nabla_{\eta_{\mathrm{r}}} \boldsymbol{f}_{\mathrm{r}} - \boldsymbol{L}\nabla_{\eta_{\mathrm{r}}} f_n\\
&\triangleq \boldsymbol{A}_{\mathrm{r}} - Lc_{\mathrm{r}} \in \boldsymbol{R}^{(n-1)\times(n-1)}
\end{aligned} \quad (41)$$

To keep the eigenvalues of the observer invariant, we choose a characteristic equation for the estimator, denoted by $\alpha_{\mathrm{e}}(s)$, that locates the eigenvalues in the left half of the complex plane and reflects the desired speed of the response:

$$\alpha_{\mathrm{e}}(s) = s^n + \alpha_{n-1}s^{n-1} + \cdots + \alpha_1 s + \alpha_0 = 0 \quad (42)$$

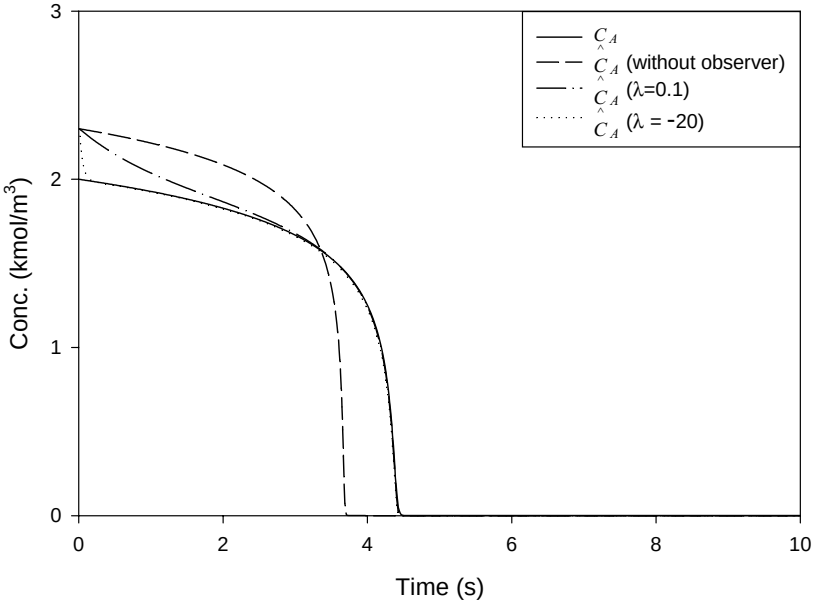

Fig. 7. Actual and estimated values of the state variable based on the open-loop and closed-loop observer for the batch reactor system.

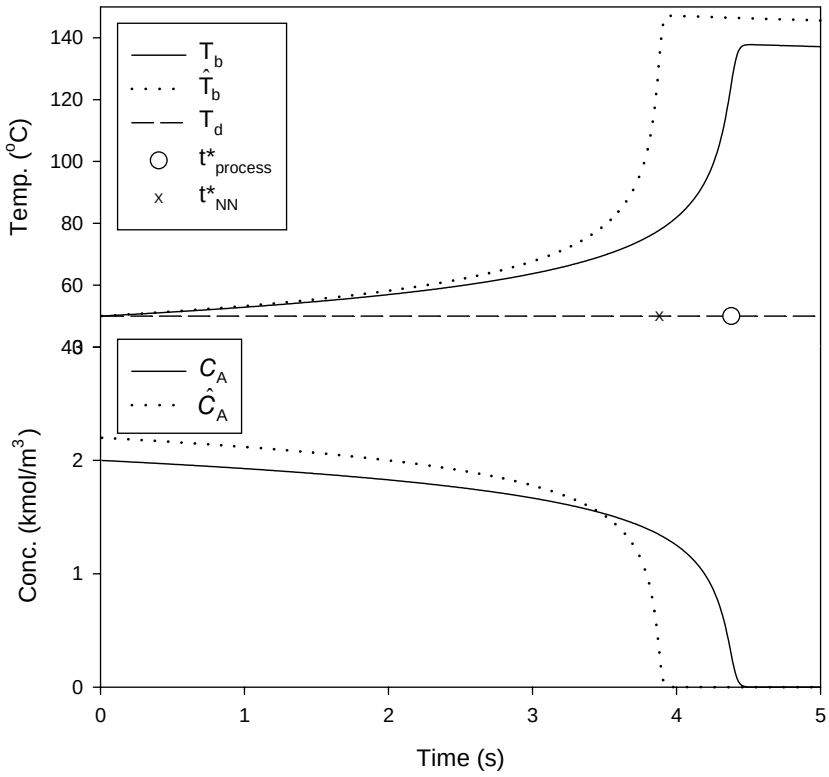

Fig. 8. Performance of the detecting scheme (Fig. 1) without observer for time profiles of T_b, $\hat{T}_b$, C_A, $\hat{C}_A$ ($C_{A_0} = 2$, $\hat{C}_{A_0} = 2.2\,\mathrm{kg\,m^{-3}}$, $T_{b_0} = \hat{T}_{b_0} = 50\,^{\circ}\mathrm{C}$) for the batch reactor system.

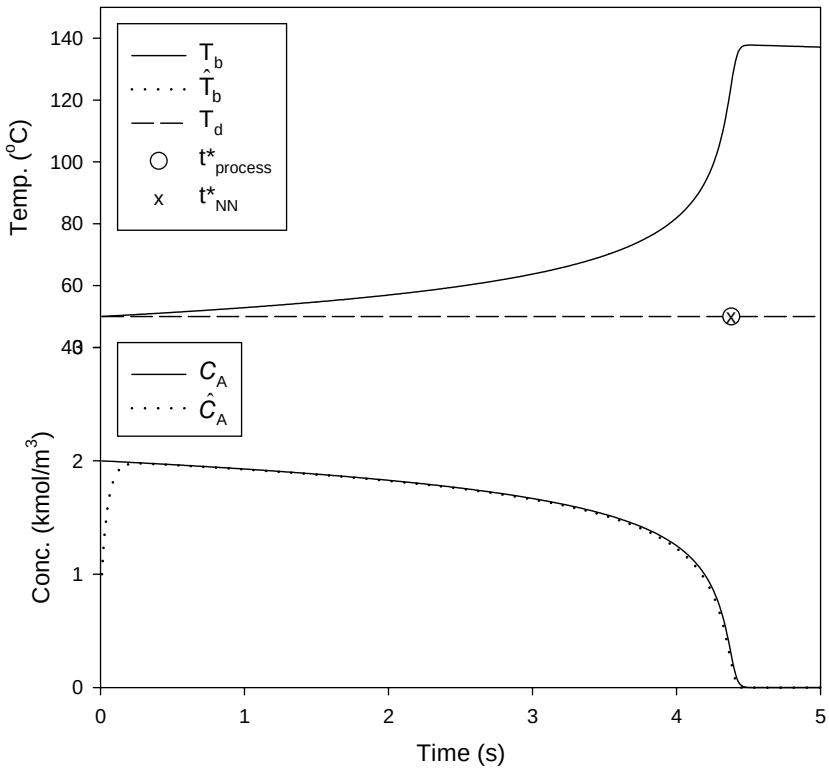

Fig. 9. Performance of the detecting scheme (Fig. 1) with observer for the time profiles of T_b, C_A, $\hat{C}_A$ ($C_{A_0} = 2$, $\hat{C}_{A_0} = 1\,\mathrm{kg\,m^{-3}}$, $T_{b_0} = \hat{T}_{b_0} = 50\,^{\circ}\mathrm{C}$) for the batch reactor system.

Then the observer gain $\boldsymbol{L}$ is calculated to satisfy

$$|s\boldsymbol{I} - \boldsymbol{A}_\mathrm{r} + L c_\mathrm{r}| = \alpha_\mathrm{e}(s) \tag{43}$$

Note the similarity of this design problem with that of pole placement [9]. Then Ackermann's formula for pole placement can be applied to the design of the state estimator, with the resulting formula

$$\boldsymbol{L} = \alpha_\mathrm{e}(\boldsymbol{A}_\mathrm{r}) \begin{bmatrix} c_\mathrm{r} \\ c_\mathrm{r}\boldsymbol{A}_\mathrm{r} \\ \vdots \\ \boldsymbol{c}_\mathrm{r}\boldsymbol{A}_\mathrm{r}^{n-1} \end{bmatrix}^{-1} \begin{bmatrix} 0 \\ 0 \\ \vdots \\ 1 \end{bmatrix} \tag{44}$$

5.1. Application of the reduced order observer with variable gain to the processes

Adopting the temperature of the reacting medium as the available measurement, the reduced order observer was applied to estimate the immeasurable concentration of the reactants in the batch reactor. Given an initial incorrect concentration $\hat{C}_{\mathrm{A}_0} = 2.3\ \mathrm{kmol\,m^{-3}}$ instead of the real initial concentration $C_{\mathrm{A}_0} = 2\ \mathrm{kmol\,m^{-3}}$, the performance of the reduced order observer with different assigned eigenvalues λ ($\lambda = -1$ and -20) as compared to that of an open-loop observer is shown in Fig. 7. One can find that the reduced order observer with proper assigned eigenvalues can track $C_\mathrm{A}(t)$ quickly. Similar performance of the reduced order observer can be found in the CSTR.

6. Integration of the state observer and the neural network for early detection of hazardous states

The integrated system for the on-line detection of hazardous states was carried out as follows: (1) at $t = 0$, the built FNN used the initial state of the observer ($\hat{C}_{\mathrm{A}_0}$ and

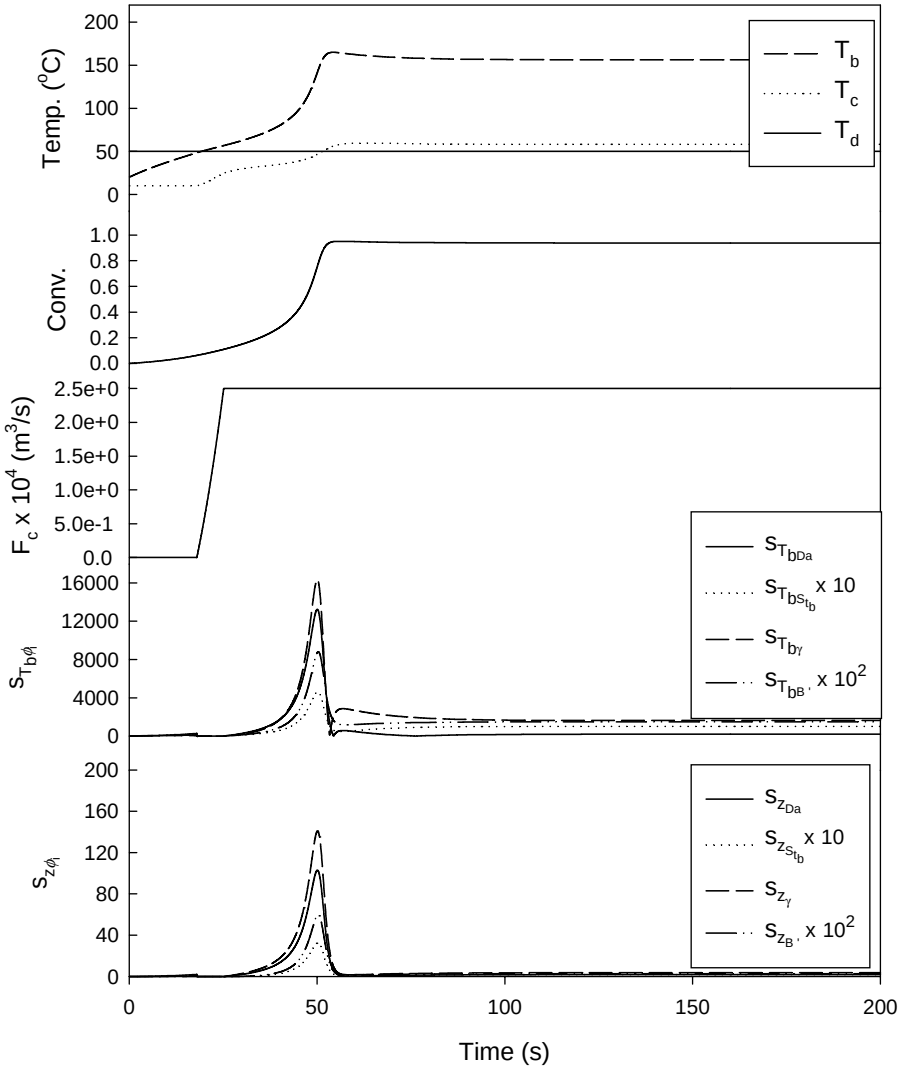

Fig. 10. Time profiles of T_b, T_c, z, $s_{T_\mathrm{b}\varphi_\mathrm{i}}$, $s_{z_{\varphi_\mathrm{i}}}$ ($T_{\mathrm{b}_0} = 70\,^\circ\mathrm{C}$, $C_{\mathrm{A}_0} = 3\,\mathrm{kg\,m^{-3}}$) developing in the CSTR.

T_{b_0}) to predict the results of the parametric sensitivity analysis and the observer started to estimate the states of the process $\hat{C}_A(t + \Delta t)$, (2) at $t = t + \Delta t$, with $T_{b_0} = T_b(t)$ and $C_{A_0} = \hat{C}_A(t + \Delta t)$, the results of the parametric sensitivity analysis were predicted by the built FNNs, and (3) went to (2). Because the concentration of the reactant estimated by the reduced order observer requires several integration steps to arrive at the correct states of the process, the built FNNs cannot provide correct results of the parametric sensitivity analysis till the observer provides the correct state ($C_A(t)$). To ascertain when the results of the parametric sensitivity analysis are reliable, the next equation can be applied:

$$t^*\big|_{t=t_1} + \Delta t\big|_{t=t_1} \approx t^*\big|_{t=t_2} + \Delta t\big|_{t=t_2} \quad (45)$$

That is, when the output of the observer tracks the true state, $t^*|_{t=t} + \Delta t|_{t=t}$ calculated by the FNNs should converge to the same value at different time instants. In the above equation, $t^*|_{t=t}$ is the time required from the time instant t to the time when the reaction is going to be a thermal runaway, and $\Delta t|_{t=t}$ $(= t - t_0)$ is the time span from the initial time of the reaction.

The performance of the detecting scheme (Fig. 1) was first examined in the batch reactor operation. Fig. 8 shows the performance of the detecting scheme given in Fig. 1 with an open-loop observer. One can find that based on an incorrect concentration of the reactant provided by the open-loop observer ($\hat{C}_{A_0} = 2.2\,\text{kmol m}^{-3}$; $C_{A_0} = 2.0\,\text{kmol m}^{-3}$), the built FNNs cannot predict the correct time for a thermal runaway. If the reduced-order closed-loop observer is provided, the built FNNs can predict the correct time (about 4.5 s after the start up of the batch reactor) for a thermal runaway as shown in Fig. 9. In this case, there exists a larger mismatch of the initial concentration ($\hat{C}_{A_0} = 1.0\,\text{kmol m}^{-3}$; $C_{A_0} = 2.0\,\text{kmol m}^{-3}$) but the performance of the detecting scheme works properly. In this case, the detecting scheme developed can tackle the process with a short response time; it is expected to be workable in the batch process with a longer response time. As explained in Section 1, the detecting scheme developed in this work can save the on-line computation time for the integration of dynamic equations governing the parameter sensitivity analysis; therefore, the prediction can be obtained much faster.

The detecting scheme can also be applied to the CSTR operation properly as shown in Figs. 10 and 11. In Fig. 10, the CSTR was operated under closed-loop control and the parametric sensitivity analysis was executed only during the time $F_c = F_{c_{min}}$ and $F_c = F_{c_{max}}$. In this figure, the peaks of $s_{T_c\varphi_i}$ are not significant compared with those of $s_{T_b\varphi_i}$ and $s_{z_{\varphi_i}}$; therefore, there are not depicted in the figure. At the first time F_c reached $F_{c_{max}}$, the detecting scheme can predict the correct time (about 30 s later) for a thermal runaway as shown in Figs. 10 and 11. Successful demonstrations via simulation both in the batch reactor and CSTR systems

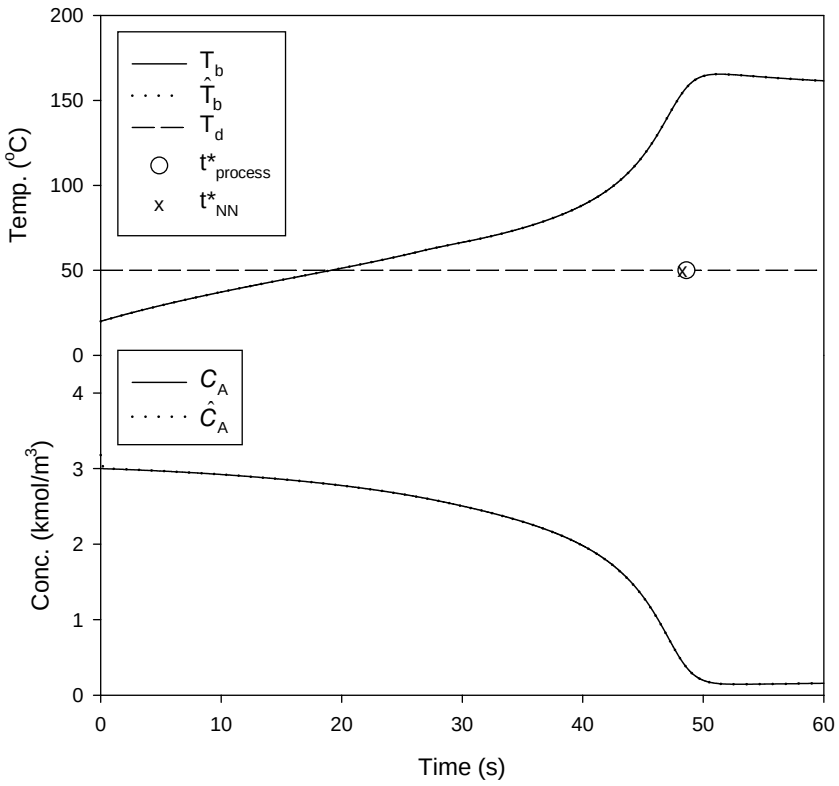

Fig. 11. Performance of the detecting scheme (Fig. 1) with observer for the time profiles of T_b, C_A, $\hat{C}_A$ ($C_{A_0} = 3$, $\hat{C}_{A_0} = 3.2\,\text{kg m}^{-3}$, $T_{b_0} = \hat{T}_{b_0} = 70\,^\circ\text{C}$) for the CSTR system.

suggest the application of the detecting scheme to the real process.

7. Conclusions

In this study, the extension of off-line parametric sensitivity analysis to the on-line closed-loop operation of chemical reactor systems was evaluated. If the reactor is operated in the safe condition space, the sensitivities present the peak at different times, whereas in runaway conditions, the maxima appear distinctly at the same time, regardless of the particular state variable or the particular parameter chosen for the definition of the sensitivity. To execute a parametric sensitivity analysis, a reliable system model with correct model parameters and initial states is indispensable. In this study, correct model structure and model parameters were assumed, but the initial states may be different from those of the actual reacting system due to incorrect dosing. A reduced order state observer with variable gain was applied to estimate the correct states for parametric sensitivity analysis. The closed-loop reduced observer can estimate the correct reactant concentration in a short time.

When the input parameters vary, the parametric sensitivity analysis can be executed on-line by repeated integration of the system equations. However, to reduce the computation burden, two FNNs built on the basis of the off-line parametric sensitivity analysis were applied to analyze the parametric sensitivity on-line. Using the first neural network, the inputs are the initial temperature and initial concentration of the reacting system; the output is zero or one (parameter insensitive or sensitive, respectively). If the reactor is operated in a parameter sensitive space as predicted from the first neural network, a second neural network is then applied. Using the temperature and concentration as inputs, the second neural network outputs the time that the maximal parametric sensitivities to the independent parameters are to be induced. These two neural networks can be applied to conduct the parametric sensitivity analysis quickly and correctly.

Finally, the integration of the developed state observer and the neural networks was applied to execute the parametric sensitivity analysis for an early detection of hazardous states both in the batch reactor and CSTR systems. By a fast-converged estimation of the initial conditions and repeated application of the neural networks, the parametric sensitivity analysis can be evaluated quickly and correctly in the face of any on-line variation of system parameters. Therefore, early detection of the parametric sensitive operating conditions could be provided and remedial measures could be taken by the operator to prevent the reacting system from a possible runaway in time.

Acknowledgements

We thank the National Science Council (Grant NSC 89-CPC-7-036-002) and Dr. T.S. Lin, President of Tatung University, Taipei, Taiwan, ROC, for all the support conducive to the completion of this work.

References

[1] E.D. Gilles, H. Schuler, Ger. Chem. Eng. 5 (1982) 69.
[2] P. Hugo, J. Steinbach, F. Stoessel, Chem. Eng. Sci. 43 (1988) 2147.
[3] R.M. Chemburkar, M. Morbidelli, A. Varma, Chem. Eng. Sci. 41 (1986) 1647.
[4] M. Morbidelli, A. Varma, Chem. Eng. Sci. 43 (1988) 91.
[5] M.A. Alós, J.M. Zaldivar, F. Strozzi, R. Nomen, J. Sempere, Chem. Eng. Technol. 19 (1996) 222.
[6] M.A. Alós, T. Obertopp, M. Mangold, E.D. Gilles, Chemische Reaktionen-Erkennung und Beherrschung Sicherheitstechnisch Relevanter Zustaende und Ablaeufe, Prax. Sicherheitstech. 4 (1997) 293.
[7] J. Adler, J.W. Enig, Combust. Flame 8 (1964) 97.
[8] M. Soroush, Chem. Eng. Sci. 52 (1997) 387.
[9] C.L. Phillips, R.D. Harber, Feedback Control Systems, third ed., P.H. Hall International Inc.